

Hydroquinone analog 4-[(Tetrahydro-2H-pyran-2-yl) oxy] phenol induces C26 colon cancer cell apoptosis and inhibits tumor growth *in vivo*

QIGEN DU^{1*}, GUANG XIN^{1*}, HAI NIU^{1,2} and WEN HUANG¹

¹Laboratory of Ethnopharmacology, Regenerative Medicine Research Center, West China Hospital, West China Medical School and Institute for Nanobiomedical Technology and Membrane Biology, Sichuan University, Chengdu, Sichuan 610041; ²College of Mathematics, Sichuan University, Chengdu, Sichuan 610064, P.R. China

Received March 27, 2014; Accepted December 2, 2014

DOI: 10.3892/mmr.2015.3300

Abstract. The 4[(Tetrahydro-2H-pyran-2-yl) oxy] phenol (XG-d) hydroquinone analog, is found in *Vaccinium vitis-idaea* L. Although it is known for its antioxidant properties and high level of safety, its antitumor activity remains to be elucidated. In the present study, the anticancer effect of XG-d was determined *in vitro* and *in vivo*. The cytotoxicity of XG-d against C26 murine colon carcinoma cells was found to occur in a time- and concentration-dependent manner, whereas little effect was observed in the two normal cell lines (HK-2 and L02) investigated. Oral administration of XG-d (100 mg/kg) had effects on the tumor growth of tumor-bearing mice. Furthermore, marked apoptosis was observed using Hoechst 33258 staining and flow cytometric analysis with annexin V/propidium iodide double staining. XG-d also downregulated the expression of B-cell lymphoma 2 (Bcl-2), increased the expression levels of Bcl-2-associated X protein and activated caspase-9, caspase-3 and poly(adenosine diphosphate-ribose) polymerase. The present study demonstrated for the first time, to the best of our knowledge, that XG-d inhibited cancer cell growth via the induction of apoptosis and was also able to inhibit tumor growth *in vivo*. These results demonstrated that XG-d may be used as a potential natural agent for cancer therapy with low toxicity.

Introduction

Colorectal cancer (CRC) is a significant health problem worldwide, which has become the second most common cause of cancer-associated mortality (1,2). Every year, there are >1,200,000 cases of CRC diagnosed worldwide, the majority of cases occurring in developing countries (3). Surgical resection remains the first choice for CRC therapy; however, the patients are subjected to significant pain during the recovery process (4). Furthermore, due to the high risk of CRC relapse, surgery is frequently combined with chemotherapy and radiation therapy (5). Several anticancer drugs have been clinically applied in the treatment of CRC, including irinotecan, Tomudex and oxaliplatin (6), of which 5-fluorouracil (5-FU) is the most widely prescribed. However, clinical insufficiencies occur as a result of 5-FU resistance and severe side effects (7,8). Therefore, the identification of a safer and more effective drug, which can inhibit the progression of colon cancer is required.

Apoptosis describes the mechanism by which cells undergo programmed death in order to control cell proliferation or in response to DNA damage (9). There are two main apoptotic pathways, termed the extrinsic and intrinsic pathway (10). The intrinsic pathway refers to the mitochondrial pathway, in which caspase activation is closely linked to mitochondrial changes, mediated by members of the B-cell lymphoma 2 (Bcl-2) family (11,12). The Bcl-2 family proteins are divided into pro-apoptotic and anti-apoptotic proteins, which balance the levels of apoptosis amongst cells (13-15).

A number of studies have demonstrated that various herbal medicines have potential antitumor activities (16-18). 4-[(Tetrahydro-2H-pyran-2-yl)oxy] phenol (XG-d) is a hydroquinone analog, which exists in *Vaccinium vitis-idaea*, which is an ericaceous plant used for the treatment of dysuria, gonorrhoea and diarrhoea (19). It has been reported that the leaves and berries of the plant have antiviral and anti-inflammatory effects (20), however, to the best of our knowledge, no previous studies have investigated the antitumor effects of XG-d in cancer.

In the present study, the anticancer activity of XG-d was investigated in the C26 murine colon carcinoma cell line and the effects of XG-d on a tumor-bearing mouse model were

Correspondence to: Professor Wen Huang, Laboratory of Ethnopharmacology, Regenerative Medicine Research Center, West China Hospital, West China Medical School and Institute for Nanobiomedical Technology and Membrane Biology, Sichuan University, 1 Ketuan 4th Road, Gaopeng Avenue, Hi-Tech Zone, Chengdu, Sichuan 610041, P.R. China
E-mail: huangwen@scu.edu.cn

*Contributed equally

Key words: hydroquinone analog, proliferation, apoptosis, colon cancer, antitumor

evaluated. The aim was to demonstrate the potential antitumor activity of XG-d *in vitro* and *in vivo* and contribute to the development of a novel potential antitumor drug with low toxicity.

Materials and methods

Chemicals reagents. XG-d, with a purity >99%, was purchased from Shanghai Boyle Chemical Co., Ltd (Shanghai, China). Standard stock solution (10 mg/ml) were prepared with dimethyl sulfoxide (DMSO; Sigma-Aldrich, St. Louis, MO, USA) and diluted to the indicated concentrations with basal medium [RPMI-1640 (Gibco Life Technologies, Carlsbad, CA, USA), Dulbecco's modified Eagle's medium (DMEM; Invitrogen Life Technologies, Grand Island, NY, USA) and DMEM/F-12 medium (HyClone, GE Healthcare Life Science, Little Chalfont, UK)] prior to each experiment. 5-FU was purchased from Sinopharm Chemical Reagent Co., Ltd (Shanghai, China). Mouse monoclonal anti-GAPDH (1:5,000-10,000; G8795) were purchased from Sigma-Aldrich. The following primary antibodies were purchased from Cell Signaling Technology, Inc. (Beverly, MA, USA): Rabbit polyclonal anti-caspase-3 (1:1,000; #9662S), mouse monoclonal anti-caspase-9 (1:1,000; #9508S), rabbit polyclonal anti-poly(adenosine diphosphate ribose) polymerase (PARP; 1:1,000; #9542S), rabbit monoclonal anti-Bcl-2 (1:500; #2870S) and rabbit polyclonal anti-Bax (1:1,000; #2772S). Horseradish peroxidase-conjugated goat anti-mouse immunoglobulin (Ig)G (1:5,000; sc-2005) and goat anti-rabbit IgG (1:5,000; sc-2004) were purchased from Santa Cruz Biotechnology Inc. (Santa Cruz, CA, USA).

Cell lines and culture. The A549 human lung carcinoma cell line, HK-2 human proximal tubule epithelial cell line and HT-29 human colon carcinoma cell line were obtained from The American Type Culture Collection (Manassas, VA, USA). The C26 murine colon carcinoma cell line and L02 human liver cell line were purchased from the Cell Bank of the Shanghai Institute of Biochemistry and Cell Biology, Chinese Academy of Sciences (Shanghai, China). The A549 and HT-29 cell lines were cultured in DMEM, the C26 and L02 cell lines were maintained in RPMI-1640 medium and the HK-2 cell line was cultured in DMEM/F-12 medium. All cell culture mediums were supplemented with 10% fetal bovine serum (Gibco, Auckland, New Zealand), 100 U/ml penicillin and 100 µg/ml streptomycin (HyClone) at 37°C in a humidified atmosphere containing 5% CO₂.

Animals. Female BALB/c mice (4-6 weeks old) with body weights ranging from 18-22 g were purchased from Chengdu Dashuo Biotechnology Co, Ltd (Chengdu, China). The present study was approved by the ethics committee of the Institutional Animal Care and Treatment Committee of Sichuan University (Sichuan, China). The animal room was controlled to maintain temperature (22±2°C), light (12 h light/dark cycles) and humidity (50±10%).

Cell viability assay. Cell viability was measured using a cell counting kit-8 (CCK-8) kit (Dojindo, Tokyo, Japan), according to the manufacturer's instructions. Briefly, the cells were seeded into 96-well culture plates (Costar Corning, Inc., Corning, NY, USA) at a density of 4,000 cells/well. Following incubation

overnight, the cells were treated with various concentrations of XG-d (2.5, 5, 10, 20 or 40 µg/ml). DMSO (<0.1%) was used as an untreated control. Following 48 h of incubation at 37°C, 10 µl CCK-8 solution was added to each well and incubated for 3 h, prior to the measurement of the absorbance at 450 nm using a SpectraMax M5 microplate reader (Molecular Devices, LLC, Sunnyvale, CA, USA).

Hoechst staining. The cells were washed with phosphate-buffered saline (PBS; Solarbio Science and Technology Co., Ltd, Beijing, China) and fixed with 4% paraformaldehyde (HyClone) for ~20 min at room temperature. The fixed cells were subsequently stained with Hoechst 33258 (Biyuntian Biotechnology Co., Shanghai, China) at 37°C for 15 min, washed with PBS twice and the changes in the nuclei were examined using a fluorescence microscope (uX71; Olympus Corp., Tokyo, Japan).

Cell cycle analysis. In order to evaluate the cell cycle distribution following drug treatment, the DNA contents were analyzed using flow cytometry. Following treatment with the drug for 24 h, the cells were harvested, washed once with PBS and fixed using 70% ethanol (Sigma-Aldrich) at 4°C overnight. Following centrifugation at 600 x g for 5 min, the cells were analyzed using a Cell Cycle and Apoptosis analysis kit (Biyuntian Biotechnology Co., Shanghai, China), according to the manufacturer's instructions. The cells were analyzed using a fluorescence-activated cell sorting (FACS) can flow cytometer (Navios; Beckman Coulter, Brea, CA, USA).

Transmission electron microscopy. XG-d was prefixed with a mixed solution of 3% glutaraldehyde (Sinopharm Chemical Reagent Co., Ltd) and then post-fixed with 1% osmium tetroxide, dehydrated in series of acetone solutions, infiltrated in Epox 812 (Beijing Zhongjingkeyi Technology Co., Ltd., Beijing, China) for approximately 3 h and were subsequently embedded. The semi-thin sections (0.6~0.8 µm; used in for optical positioning) were cut with a slicer and stained with methylene blue (Sigma-Aldrich) and ultra-thin sections (<0.1 µm; used for observation) were cut using a diamond knife (Beijing Zhongjingkeyi Technology Co., Ltd.), then stained with uranyl acetate and lead citrate. Sections were then examined using a transmission electron microscope (H-600IV; Hitachi, Tokyo, Japan).

Annexin V/propidium iodide (PI) double staining assay. The C26 cells were treated with XG-d for 24 h, harvested and washed three times with PBS. The apoptotic assay was performed using an annexin V-fluorescein isothiocyanate (FITC)/PI apoptosis kit (KeyGEN, Nanjing, China), according to the manufacturer's instructions. The cells were resuspended in 500 µl binding buffer and 5 µl Annexin V-FITC and PI were added. The cells were subsequently incubated for 15 min in the dark and the samples were measured using a fluorescence activated cell sorting (FACS) can flow cytometer (Beckman Coulter).

Western blot analysis. The cells were washed with cold PBS and lysed in radioimmunoprecipitation assay lysis buffer (Biyuntian Biotechnology Co., Shanghai, China), containing 50 mM Tris-HCl (pH 7.4), 150 mM NaCl,

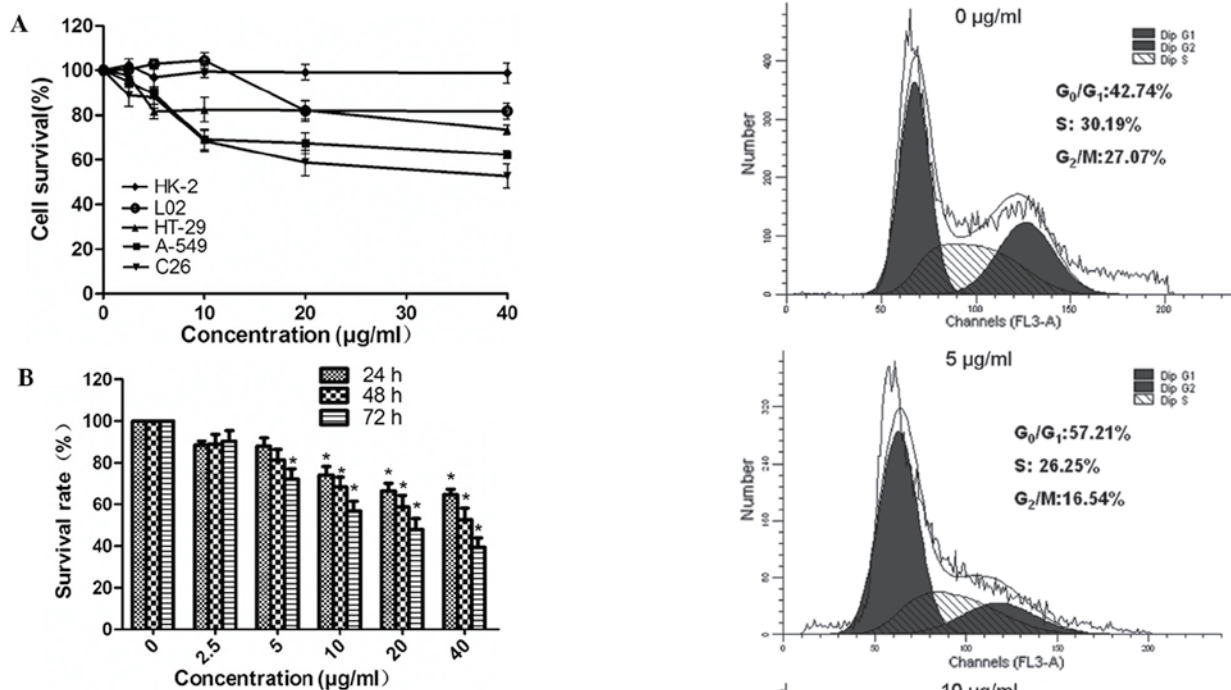


Figure 1. XG-d effects on cell survival. (A) HK-2, L-02, HT-29, A-549 and C26 cells were treated with the indicated concentrations of XG-d for 48 h. (B) C26 cells were treated with the indicated concentrations of XG-d for different durations. XG-d inhibited the C26 cell proliferation in a time- and dose-dependent manner. Results are expressed as the mean \pm standard error of the mean of three separate experiments. * $P < 0.05$, vs. control cells. XG-d, 4-[(Tetrahydro-2H-pyran-2-yl)oxy] phenol.

1% TritonX-100, 1% sodium deoxycholate, 0.1% SDS, 1 mM sodium orthovanadate, 1 mM EDTA, 1 mM phenylmethanesulfonylfluoride and 50 mM NaF for 20 min on ice. Subsequently, the cell lysates were centrifuged for 10 min at 12,000 \times g at 4°C. The total protein in the supernatants was determined using a Bicinchoninic Acid Protein Assay kit (Biyuntian Biotechnology, Co.). Equal quantities of protein was separated by 10% SDS-PAGE and transferred onto a polyvinylidene fluoride membrane (EMD Millipore, Billerica, MA, USA) by electroblotting. The membrane was then blocked with 5% non-fat milk for 1 h and was incubated with primary antibodies for PARP (1:1,000), caspase-9 (1:1,000), caspase-3 (1:1,000), Bcl-2 (1:500), Bax (1:500) and GAPDH (1:5,000-10,000), as described above, at 4°C overnight (>18 h). Following washing, the blots were incubated with a horseradish peroxidase-conjugated goat anti-mouse and goat anti-rabbit IgG secondary antibodies (1:5,000) at room temperature for 1 h, with agitation. The reactive bands were detected by enhanced chemiluminescence using either SuperSignal West Pico Chemiluminescent Substrate (Thermo Fisher Scientific, Waltham, MA, USA) or Immobilon Western Chemiluminescent HRP Substrate (Millipore), according to the manufacturer's instructions.

Tumor growth assay. The C26 cells (1.0×10^6) were subcutaneously implanted in the right flank region of the BALB/c mice (21). Seven days following implantation, the mice with tumor sizes $>50 \text{ mm}^3$ were selected and randomly divided into three groups ($n=10$ per group), termed the vehicle control, XG-d and positive groups. These groups were treated with

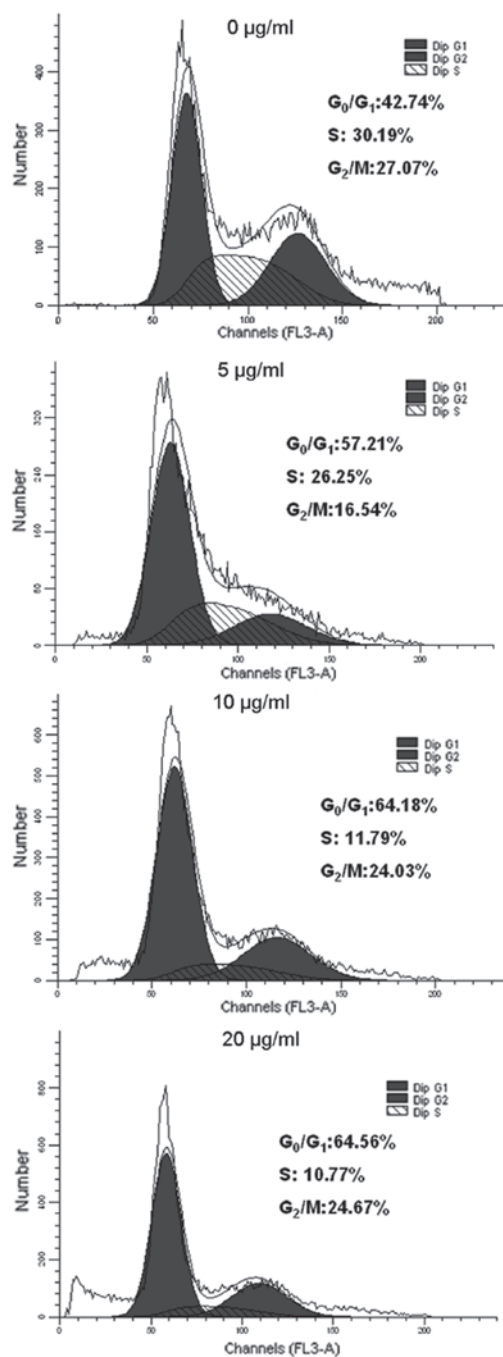


Figure 2. The effects of XG-d treatment on the cell cycle distribution of C26 cells. C26 cells were treated with various concentrations of XG-d (5, 10 or 20 µg/ml) for 24 h and analyzed by flow cytometry. The data is representative of three independent experiments. XG-d, 4-[(Tetrahydro-2H-pyran-2-yl)oxy] phenol.

0.5% carboxymethyl cellulose sodium (Aladdin Industrial, Inc., Shanghai, China), 100 mg/kg XG-d and 30 mg/kg 5-FU (Sinopharm Chemical Reagent Co., Ltd), respectively, the concentrations of which were determined in a preliminary study. Equal volumes of the drugs and vehicle were administered orally to the mice every day for 3 weeks. The body weight (MP5002 Electronic balance; Shanghai Sunny Henping Scientific Instrument Co., Ltd., Shanghai, China) and tumor size were measured twice weekly and the tumor volumes were calculated using the formula $0.52 \times a \times b^2$, where 'a' represented the long diameter and 'b' represented the short diameter. At

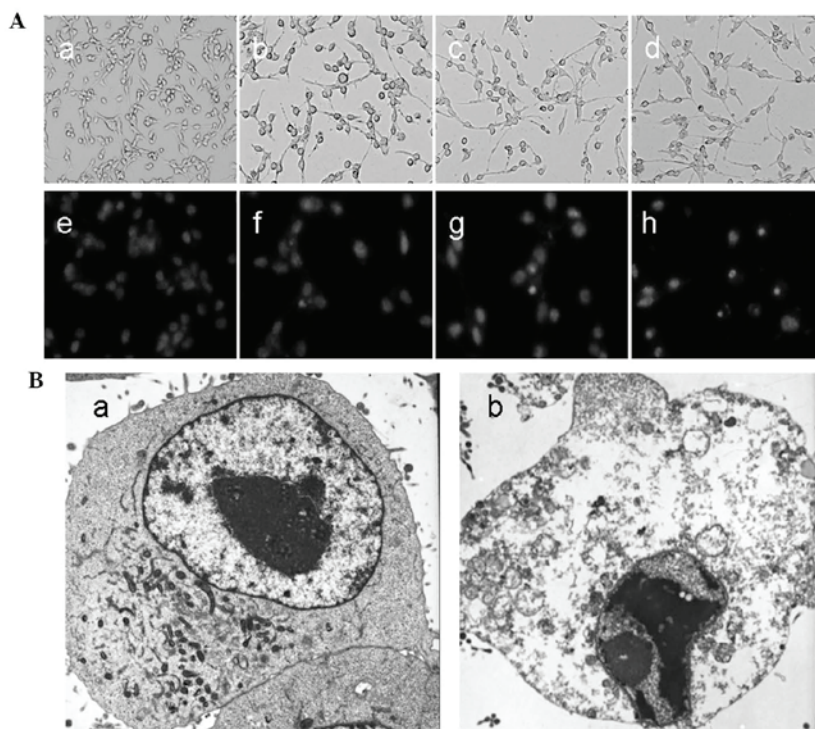


Figure 3. Cell morphology was altered following treatment with XG-d. (A) Morphological changes of C26 cells following treatment with XG-d at the indicated concentrations for 24 h (a and e, control; b and f, 5 $\mu\text{g/ml}$; c and g, 10 $\mu\text{g/ml}$; d and h, 20 $\mu\text{g/ml}$). The cells were analyzed under a phase contrast microscope with (a-d) no staining (magnification, x200) and (d-h) under a fluorescence microscope following staining with Hoechst 33258 for 15 min (magnification x400). (B) C26 cells were exposed to 20 $\mu\text{g/ml}$ XG-d for 48 h followed by observation using transmission electron microscopy. (a) control; (b) 20 $\mu\text{g/ml}$ XG-d. XG-d, 4-[(Tetrahydro-2H-pyran-2-yl)oxy] phenol.

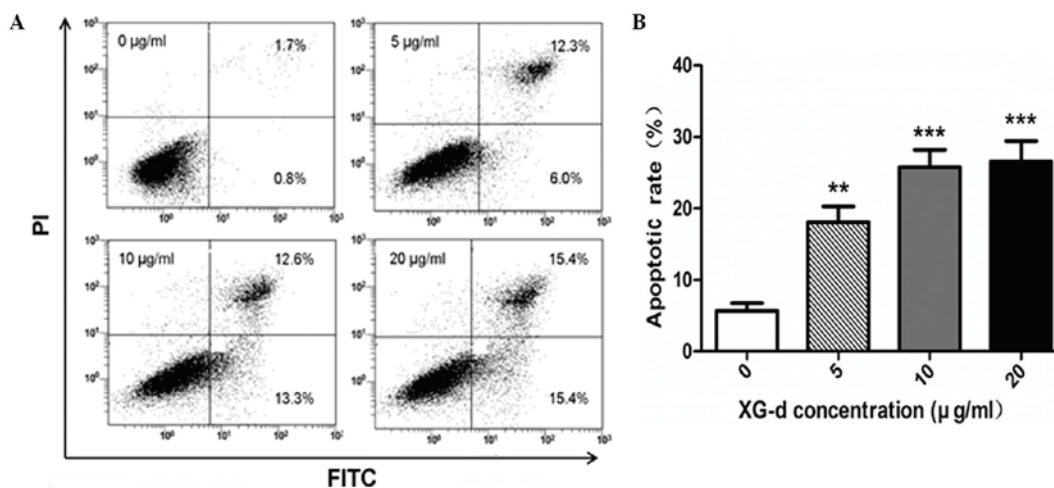


Figure 4. XG-d induces apoptosis in the C26 cells. (A) Cells were incubated with XG-d for 24 h, harvested and stained with annexin V-FITC and PI for flow cytometric analysis of apoptosis. The lower right quadrants indicate the early stage apoptotic cells and the upper right quadrants represent late apoptotic and necrotic cells. (B) Graph summarizing the effect of XG-d on the apoptotic rate of C26 cells. Values are expressed as the mean \pm standard error of the mean of three independent experiments. * $P < 0.05$, ** $P < 0.01$ and *** $P < 0.001$, vs. control group. XG-d, 4-[(Tetrahydro-2H-pyran-2-yl)oxy] phenol; FITC, fluorescein isothiocyanate; PI, propidium iodide.

the end of the treatment, the mice were sacrificed by cervical dislocation and the tumors were excised and weighed.

Statistical analysis. All the values are expressed as the mean \pm standard error of the mean. Statistical significance was analyzed by one-way analysis of variance, followed by Scheffe's test for multiple comparisons. Statistical analyses were performed using GraphPad Prism 5.0 software (GraphPad

Software, Inc., La Jolla, CA, USA). $P < 0.05$ was considered to indicate a statistically significant difference.

Results

XG-d inhibits C26 cell proliferation with low levels of toxicity on the L02 and HK-2 cells. The effects of XG-d on the proliferation of various cell lines were determined using a CCK-8 assay.

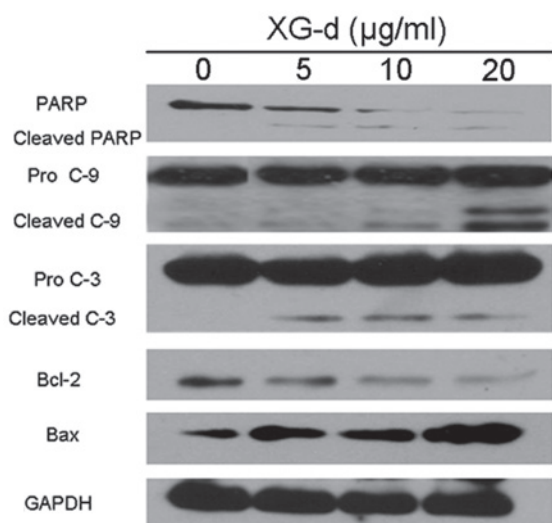


Figure 5. The effects of XG-d on the expression of apoptosis-associated proteins in the C26 cells. The cells were treated with various concentrations of XG-d for 24 h and the total protein levels were evaluated by western blot analysis. The expression levels of PARP, C-9, C-3, Bcl-2 and Bax were assessed. The results are representative of three independent experiments. XG-d, 4-[(Tetrahydro-2H-pyran-2-yl)oxy] phenol; PARP, poly(adenosine diphosphate ribose) polymerase; C-9, caspase-9; Bcl-2, B-cell lymphoma 2; Bax, Bcl-2-associated X protein.

The cell viability was examined in three carcinomatosis cell lines (A549, C26 and HT-29) and two normal cell lines (HK-2 and L-02), which had been treated with various concentrations of XG-d (2.5, 5, 10, 20 or 40 $\mu\text{g/ml}$) for 48 h. XG-d significantly inhibited the proliferation of the C26 cells and had less marked effects on the A549 and HT-29 cancer cell lines and the L02 and HK-2 normal cell lines (Fig. 1A). The inhibitory effect of XG-d on C26 growth at various concentrations were similar after 24 and 48 h incubation ($P>0.05$); therefore, a duration of 24 h was used in the subsequent investigations (Fig. 1B).

XG-d induces C26 cell cycle arrest in the G_0/G_1 phase. DNA cell cycle analysis was used to examine the effects of XG-d on the growth of the C26 cells. The C26 cells were incubated with various concentrations of XG-d for 24 h. As shown in Fig 2, compared with the control group, the G_0/G_1 phase was significantly increased between 42.74 and 64.56%, while the number of cells in the S phase gradually decreased between 30.19 and 10.77% in the XG-d-treated group with increasing XG-d concentration.

Cell morphological assessment. In order to investigate how XG-d inhibited cell viability, cell morphology was examined. As shown in Fig. 3A, morphological changes were observed in the C26 cells following treatment with XG-d for 24 h. Notably, the control cells emitted light blue fluorescence and the nuclei were round, suggesting that the chromatin was equivalently distributed. However, the XG-d-treated cells exhibited shrinkage, chromatin congregation and nuclear fragmentation.

Subsequently, a transmission electronic microscope was used to identify morphological changes in the ultrastructure of the C26 cells. No clear damage was observed in the control group (Fig. 3Ba), however, the XG-d-treated group exhibited

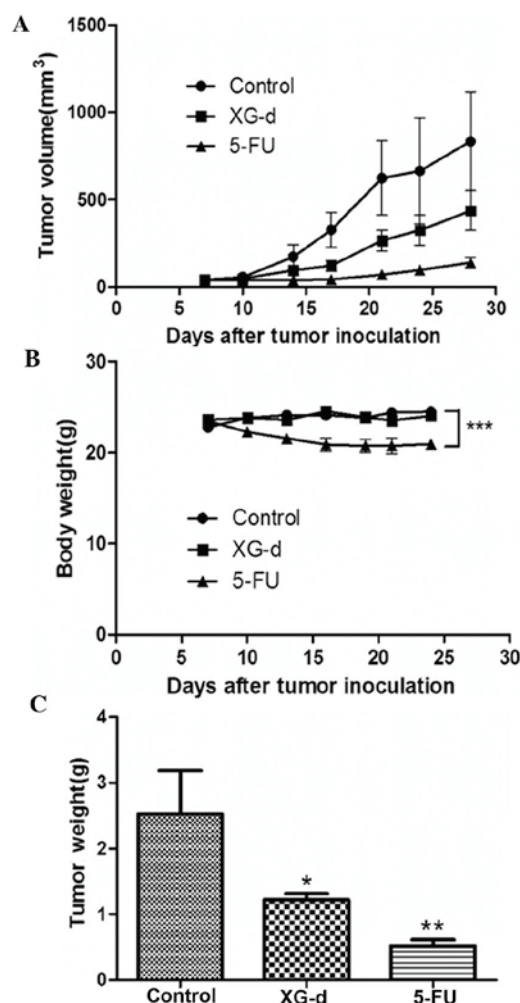


Figure 6. XG-d inhibits tumor growth in a tumor bearing-mouse model. (A) XG-d suppressed tumor growth *in vivo* compared the vehicle control group. (B) Analysis of body weight to determine the toxicity of the treatment. No significant difference was observed between the body weights of the control and XG-d groups, however, the body weights of the 5-FU group was significantly decreased following XG-d treatment. (C) Average tumor weight following 21 days of vehicle, XG-d or 5-FU treatment. Values are expressed as the mean \pm standard error of the mean. * $P<0.05$, ** $P<0.01$ and *** $P<0.001$, compared with the control. XG-d, 4-[(Tetrahydro-2H-pyran-2-yl)oxy] phenol; 5-FU, 5-fluorouracil.

chromatin congregation, nucleic degeneration and cytoplasm shrinkage, while the nuclear envelope and cell membrane remained intact (Fig. 3Bb). These results suggested that XG-d was capable of inducing apoptosis in the C26 cells.

XG-d induces apoptosis. Flow cytometric analysis using an Annexin V-FITC apoptosis kit was used to identify the levels of apoptosis induced by XG-d in the C26 cells. As indicated in Fig. 4A, the C26 cells were exposed to various concentrations of XG-d (5, 10 or 20 $\mu\text{g/ml}$) for 24 h. The percentage of early apoptotic cells increased to 15.4%, while the percentage of late apoptotic cells and necrotic cells increased to 15.4% following treatment with 20 $\mu\text{g/ml}$ XG-d, compared with the control group. A significant increase in the apoptotic rate was induced in the XG-d treated groups compared with the untreated group ($P<0.05$; Fig. 4B). The results indicated that XG-d induced apoptosis in the C26 cells.

XG-d effects the expression of apoptosis-associated proteins. To evaluate the potential pathways responsible for the effects of XG-d, the expression of key apoptosis-associated proteins in C26 cells were examined (Fig. 5). PARP, a nuclear enzyme involved in DNA repair, was cleaved into 89 kDa fragments. Caspase-9 and caspase-3 were also cleaved and accumulated following XG-d treatment. Furthermore, the expression of Bcl-2 was decreased, while the expression levels of Bax were upregulated. These results indicated that XG-d induced the caspase-dependent and mitochondria-mediated apoptotic pathways.

XG-d inhibits colon tumor growth in vivo. In the present study, a mouse tumor model of colon cancer was used to examine the effect of XG-d on tumor growth *in vivo*. Each mouse was subcutaneously injected with 1.0×10^6 C26 cells. Following establishment of the tumor ($\sim 50 \text{ mm}^3$), the anti-tumor effects of oral administration of 100 mg/kg XG-d to the mice were evaluated. Oral administration of 5-FU (30 mg/kg) was used as a positive control and oral administration of 0.5% carboxymethyl cellulose sodium was used as the normal control. As indicated in Fig. 6A, after 3 weeks treatment, the average tumor size in the vehicle control group was $834.8 \pm 284.1 \text{ mm}^3$, whereas the average tumor size in the XG-d- and 5-FU-treated groups were 436.8 ± 114.1 and $138.9 \pm 31.3 \text{ mm}^3$, respectively. The weight of the mice was also measured over the course of the treatment period. No significant difference was observed between the body weights of the vehicle control or XG-d-treated groups, however, the body weights of the mice in the 5-FU-treated group were decreased (Fig. 6B). The tumor weight of the XG-d- and 5-FU-treated mice after 3 weeks of treatment were significantly reduced compared with that of the vehicle control (Fig. 6C). These results revealed that the oral administration of XG-d inhibited C26 cell tumor growth.

Discussion

In the last 20 years, herbal plant compounds have been studied in order to elucidate their potential antitumor activity (22). XG-d is an effective tyrosinase inhibitor, which is frequently used to whiten skin (23,24). In the present study, it was revealed that XG-d potentially suppresses C26 cell proliferation *in vitro*; in addition, these results indicated that XG-d induces C26 cell apoptosis in a dose- and time-dependent manner. Furthermore, XG-d upregulated the expression of Bax, downregulated the expression of Bcl-2 and activated caspase-9, caspase-3 and PARP proteins.

Inducing cellular apoptosis is an important strategy in treating cancer. The anticancer action of numerous chemotherapeutic agents have been found to cause cell death via the induction of apoptosis (25,26). Caspases have a critical role in apoptosis. In response to apoptotic stimuli, the mitochondrial membrane becomes permeable, leading to the release of cytochrome-C into the cytosol. Subsequently, cytochrome-C activates the caspase-9 and caspase-3 pro-enzymes, inducing a caspase signaling cascade and resulting in cell apoptosis (27,28). Among the known members of the interleukin-1-converting enzyme family of proteases, the key component of the apoptotic mechanism is caspase-3 (29). Caspase-3 cleaves multiple

cellular proteins, including PARP, the cleaved form of which is associated with apoptosis (30). In the present study caspase-9 and caspase-3 were found to be activated, while PARP was cleaved. These findings suggested that XG-d increased the percentage of apoptotic cells in a dose-dependent manner. Therefore, XG-d may induce the apoptosis of C26 cells via the activation of caspases.

The Bcl-2 family is one of the most important regulators of apoptosis (31,32) and has a critical role in the mitochondrion-mediated pathway. In humans, >20 members of the Bcl-2 family have been identified, including Bcl-2, Bcl-XL, Bcl-1, Bax and Bcl-2-antagonist/killer 1 (33-35). Changes in the expression levels of Bcl-2, an anti-apoptotic protein, and Bax, a pro-apoptotic protein, is often used as an index of apoptosis (36,37). The results of the present study demonstrated that XG-d downregulated the expression of Bcl-2 and enhanced the activity of Bax. The ratio of Bax/Bcl-2, suggested that XG-d induced apoptosis in the C26 cells via the mitochondrial pathway.

In conclusion, the results of the present study indicated that XG-d induced cell death in the C26 cell line by activating the regulation of caspases and the Bcl-2 family member-dependent mitochondrial pathway. The cytotoxicity of XG-d against several cancer cell lines, in particular the C26 murine colon carcinoma cell line, was observed, however, it had low toxic effects on two normal human cell lines. Furthermore, the effects of XG-d on tumor growth *in vivo* revealed that XG-d may be a promising novel anticancer agent.

Acknowledgements

The present study was supported by the China National '12.5' Foundation (no. 2011BAJ07B04) and the National Natural Science Foundation of China (no. 20972105).

References

- Jemal A, Murray T, Ward E, *et al*: Cancer statistics, 2005. *CA Cancer J Clin* 55: 10-30, 2005.
- Center MM, Jemal A, Smith RA and Ward E: Worldwide variations in colorectal cancer. *CA Cancer J Clin* 59: 366-378, 2009.
- Jemal A, Bary F, Center MM, *et al*: Global cancer statistic. *CA Cancer J Clin* 61: 69-90, 2011.
- Saif MW: Targeted agents for adjuvant therapy of colon cancer. *Clin Colorectal Canc* 6:46-51, 2006.
- Macdonald JS: Adjuvant therapy of colon cancer. *CA Cancer J Clin* 49: 202-219, 1999.
- Longley DB, Harkin DP and Johnston PG: 5-fluorouracil: mechanisms of action and clinical strategies. *Nat Rev Cancer* 3: 330-338, 2003.
- Delval L and Klastersky J: Optic neuropathy in cancer patients. Report of a case possibly related to 5 fluorouracil toxicity and review of the literature. *J Neurooncol* 60: 165-169, 2002.
- Meregalli M, Martignoni G, Frontini L, *et al*: Increasing doses of 5-fluorouracil and high-dose folic acid in the treatment of metastatic colorectal cancer. *Tumori* 84: 662-665, 1998.
- Ghobrial IM, Witzig TE and Adjei AA: Targeting apoptosis pathways in cancer therapy. *CA Cancer J Clin* 55: 178-194, 2005.
- Ziegler DS and Kung AL: Therapeutic targeting of apoptosis pathways in cancer. *Curr Opin Oncol* 20: 97-103, 2008.
- Wong RSY: Apoptosis in cancer: from pathogenesis to treatment. *J Exp Clin Cancer Res* 30: 87, 2011.
- Green DR and Kroemer G: The pathophysiology of mitochondrial cell death. *Science* 305: 626-629, 2004.
- Borner C: The Bcl-2 protein family: sensors and checkpoints for life-or-death decisions. *Mol Immunol* 39: 615-647, 2003.

14. Adams JM and Cory S: The Bcl-2 apoptotic switch in cancer development and therapy. *Oncogene* 26: 1324-1337, 2007.
15. Willis SN, Fletcher J, Kaufmann T, *et al*: Apoptosis initiated when BH3 ligands engage multiple Bcl-2 homologs, not Bax or Bak. *Science* 315: 856-859, 2007.
16. Tin MM, Cho CH, Chan K, *et al*: Astragalus saponins induce growth inhibition and apoptosis in human colon cancer cells and tumor xenograft. *Carcinogenesis* 28: 1347-1355, 2007.
17. Miller K, Wang ML, Gralow J, *et al*: Paclitaxel plus bevacizumab versus paclitaxel alone for metastatic breast cancer. *New Engl J Med* 357: 2666-2676, 2007.
18. Phillips PA, Sangwan V, Borja-Cacho D, *et al*: Myricetin induces pancreatic cancer cell death via the induction of apoptosis and inhibition of the phosphatidylinositol 3-kinase (PI3K) signaling pathway. *Cancer Lett* 308: 181-188, 2011.
19. Morimoto S, Nonaka GI and Nishioka I: Tannins and related compounds. LX. Isolation and characterization of proanthocyanidins with a doubly-linked unit from *Vaccinium vitis-idaea* L. *Chem Pharm Bull* 36: 33-38, 1988.
20. Fokina GI, Roïkhel' VM, Frolova MP, *et al*: The antiviral action of medicinal plant extracts in experimental tick-borne encephalitis. *Vopr Virusol* 38: 170-173, 1993 (In Russian).
21. Tong QY, Qing Y, Shu D, *et al*: Deltonin, a steroidal saponin, inhibits colon cancer cell growth in vitro and tumor growth in vivo via induction of apoptosis and antiangiogenesis. *Cell Physiol Biochem* 27: 233-242, 2011.
22. Jeone SJ, Koh W, Kim B and Kim SH: Are there new therapeutic options for treating lung cancer based on herbal medicines and their metabolites. *J Ethnopharmacology* 138: 652-661, 2011.
23. Wang J, Zhao XZ, Qi Q, *et al*: Macranthoside B, a hederagenin saponin extracted from *Lonicera macranthoides* and its anti-tumor activities in vitro and in vivo. *Food Chem Toxicol* 47: 1716-1721, 2009.
24. Hu M, Xu L, Yin LH, *et al*: Cytotoxicity of dioscin in human gastric carcinoma cells through death receptor and mitochondrial pathways. *J Appl Toxicol* 33: 712-722, 2013.
25. Cai SX, Drewe J and Kasibhatla S: A chemical genetics approach for the discovery of apoptosis inducers: from phenotypic cell based HTS assay and structure-activity relationship studies, to identification of potential anticancer agents and molecular targets. *Curr Med Chem* 13: 2627-2644, 2006.
26. Hickman JA: Apoptosis induced by anticancer drugs. *Cancer Metastasis Rev* 11: 121-139, 1992.
27. Desagher S and Martinou JC: Mitochondria as the central control point of apoptosis. *Trends Cell Biol* 10: 369-377, 2000.
28. Gabriel B, Sureau F, Casselyn M, *et al*: Retroactive pathway involving mitochondria in electroloaded cytochrome c-induced apoptosis. Protective properties of Bcl-2 and Bcl-XL. *Exp Cell Res* 289: 195-210, 2003.
29. Maianski NA, Roos D and Kuijpers TW: Bid truncation, bid/bax targeting to the mitochondria, and caspase activation associated with neutrophil apoptosis are inhibited by granulocyte colony-stimulating factor. *J Immunol* 172: 7024-7030, 2004.
30. Nuñez G, Benedict MA, Hu Y and Inohara N: Caspases: the proteases of the apoptotic pathway. *Oncogene* 17: 3237-3245, 1998.
31. Duriez PJ and Shah G: Cleavage of poly(ADP-ribose) polymerase: a sensitive parameter to study cell death. *Biochem Cell Biol* 75: 337-349, 1997.
32. Cory S and Adams JM: The Bcl2 family: regulators of the cellular life-or-death switch. *Nat Rev Cancer* 2: 647-656, 2002.
33. Oltersdorf T, Elmore SW, Shoemaker AR, *et al*: An inhibitor of Bcl-2 family proteins induces regression of solid tumours. *Nature* 435: 677-681, 2005.
34. Murray A: Cyclin ubiquitination: the destructive end of mitosis. *Cell* 81: 149-152, 1995.
35. Antonsson B and Martinou JC: The Bcl-2 protein family. *Exp Cell Res* 256: 50-57, 2000.
36. Reed JC: Double identity for protein of the Bcl-2 family. *Nature* 387: 773-776, 1997.
37. Mirjoleit JF, Barberi-Heyob M, Didelot C, *et al*: Bcl-2/Bax protein ratio predicts 5-fluorouracil sensitivity independently of p53 status. *Br J Cancer* 83: 1380-1386, 2000.